Cell Calcium 51 (2012) 57–64

Contents lists available at SciVerse ScienceDirect

Cell Calcium

journal homepage: www.elsevier.com/locate/ceca

Split-intein mediated re-assembly of genetically encoded Ca^{2+} indicators

Stanley S.C. Wong[a], Ippei Kotera[b], Evan Mills[a], Hiroshi Suzuki[b,c], Kevin Truong[a,d,*]

[a] Institute of Biomaterials and Biomedical Engineering, University of Toronto, 164 College Street, Toronto, Ontario M5S 3G9, Canada
[b] Tanz Center for Research in Neurodegenerative Diseases, University of Toronto, 6 Queen's Park Crescent West, Toronto, Ontario M5S 3H2, Canada
[c] Department of Physiology, Faculty of Medicine, University of Toronto, 1 King's College Circle, Toronto, Ontario M5S 1A8, Canada
[d] Edward S. Rogers Sr. Department of Electrical and Computer Engineering, University of Toronto, 10 King's College Circle, Toronto, Ontario M5S 3G4, Canada

ARTICLE INFO

Article history:
Received 18 July 2011
Received in revised form 19 October 2011
Accepted 27 October 2011
Available online 30 November 2011

Keywords:
Genetically encoded calcium indicators
TN-XL
GCaMP2
Intein
C. elegans

ABSTRACT

While genetically encoded Ca^{2+} indicators (GECIs) allow Ca^{2+} imaging in model organisms, the gene expression is often under the control of a single promoter that may drive expression beyond, the cell types of interest. To enable more cell-type specific targeting, GECIs can be brought under the, control of the intersecting expression from two promoters. Here, we present the splitting and, reassembly of two representative GECIs (TN-XL and GCaMP2) mediated by the split intein from Nostoc, punctiforme (NpuDnaE). While the split TN-XL biosensor offered ratiometric Ca^{2+} imaging, it had a, diminished Ca^{2+} response relative to the native TN-XL biosensor. In contrast, the split GCaMP2, biosensor retained similar Ca^{2+} response to the native GCaMP2. The split GCaMP2 biosensor was, further targeted to the pharyngeal muscles of *Caenorhabditis elegans* where Ca^{2+} signals from feeding *C. elegans*, were imaged. Thus, we envision that increased cell-type targetability of GECIs is feasible with two, complementary promoters.

1. Introduction

Through complex and coordinated spatiotemporal changes in Ca^{2+} concentration, Ca^{2+} signalling mediates diverse and vital cellular processes such as cell migration, neurotransmitter secretion, apoptosis, differentiation and muscle contraction [1–4]. To reveal the relationship between Ca^{2+} signalling and other cellular processes, Ca^{2+} indicators are used to precisely image Ca^{2+} signals. Synthetic dyes are a class of Ca^{2+} indicators that provide excellent signal-to-noise ratio and fast kinetics [5]. For whole organism Ca^{2+} imaging over a long duration, synthetic dyes have inherent properties that make them unsuitable such as the difficulty in implanting dyes within cells, the limited lifespan of dyes and the non-specific labelling of many types of cells [5–7]. Genetically encoded Ca^{2+} indicators (GECIs) address these problems because they can be easily expressed and imaged for long durations (i.e. throughout the cell cycle) in the cells of whole organisms such as worms, flies and mice [5,6,8]. For example, GECIs were expressed in somatosensory and motor cortical neurons of intact *Caenorhabditis elegans* and *Drosophila melanogaster* to reveal that amplitudes of Ca^{2+} transients were linearly dependent on action potential numbers [9]. In addition, motor cortex neurons of mice expressing GECIs were able to be imaged over the course of months [9].

GECIs are categorized into two main groups based on the modality of detecting changes in Ca^{2+} concentration [5,6,8]: one correlates a change in Ca^{2+} concentration with a change in the fluorescence intensity of a single fluorescent protein [10]; the other, with a change in fluorescence resonance energy transfer (FRET) between two fluorescent proteins such as cyan fluorescent protein (CFP) and yellow fluorescent protein (YFP) [11]. Cell-type specific targeting of GECIs can in part be controlled by driving the expression under the regulation of a specific promoter [5,6,8] such as using the α-myosin heavy chain promoter to target GECIs to cardiac heart muscles in mice [12]. However, many cell-type specific promoters label cells beyond those of interest and to find one promoter that is completely specific is non-trivial [13]. To overcome this challenge, the expressions from the intersection of two different promoters have been utilized to target cells with increased cell-type specificity. Notably, this has been accomplished with engineered leucine zippers to reassemble green fluorescent proteins from its peptide fragments [14–16], but this approach has several drawbacks: first, the reassembly is non-covalent so the protein can unravel and separate; second, unpaired leucine zippers may non-specifically pair with other native leucine zipper containing proteins in the cell and thus interfere with normal cell function. An alternative approach is to use split inteins that are not known to have any biological function except to create a covalent bond between two peptide fragments by protein splicing.

* Corresponding author at: Edward S. Rogers Sr. Department of Electrical and Computer Engineering, University of Toronto, 10 King's College Circle, Toronto, Ontario M5S 3G4, Canada. Tel.: +1 416 978 7772; fax: +1 416 978 4317.
E-mail addresses: stanleysc.wong@utoronto.ca (S.S.C. Wong), ippei.kotera@utoronto.ca (I. Kotera), e.mills@utoronto.ca (E. Mills), hiroshi.suzuki@utoronto.ca (H. Suzuki), kevin.truong@utoronto.ca (K. Truong).

0143-4160/$ – see front matter © 2011 Elsevier Ltd. All rights reserved.
doi:10.1016/j.ceca.2011.10.006

Protein splicing is a unique auto-catalytic post-translational process where an intervening protein sequence, termed the intein domain, splices itself out and concomitantly links two flanking polypeptide sequences, the exteins, together with a native peptide bond [17–19]. This process requires no exogenous co-factors or energy [19]. In this study, we exploited the *trans*-protein splicing ability of the naturally occurring split DnaE intein from *Nostoc punctiforme* (*Npu*DnaE) due to its faster *trans*-splicing activities to reassemble GECIs [18,19]. *Trans*-splicing inteins have their intein domains separated into two N- and C-terminal precursor fragments that bind and then reconstitute both the intein and extein. By applying this phenomenon to GECIs, we have created the first reassembling of GECIs using split inteins. This system, in combination with using two different promoters, may be used to express GECIs in difficult to target cells/tissue such as the interneurons found within neural circuits. Here, we demonstrate this approach in reforming two artificially split GECIs post-translationally in mammalian cell lines and in live animals using transgenic *C. elegans*.

2. Results

2.1. NpuDnaE has splicing activity in mammalian cells

In mammalian cells expressing fluorescent proteins fused with the N-terminal fragment of *Npu* intein (*Npu*DnaE$_N$) and the C-terminal fragment (*Npu*DnaE$_C$), the *Npu*DnaE intein directed *trans*-protein splicing as observed by distinct subcellular localizations of the fluorescent proteins. The fusion protein *Npu*DnaE$_C$-Venus was created as the tandem fusion of *Npu*DnaE$_C$ and the YFP mutant Venus [20], while Lyn-Ceru-*Npu*DnaE$_N$-mRFP1 as the tandem fusion of the plasma membrane localization signal from Lyn [18,19], CFP mutant Cerulean [21], *Npu*DnaE$_N$ and monomeric red fluorescent protein [22] (Fig. 1A). In HeLa cells expressing *Npu*DnaE$_C$-Venus or Lyn-Ceru-*Npu*DnaE$_N$-mRFP1 alone, as expected, the cytoplasm was yellow fluorescent and the plasma membrane was cyan–red fluorescent, respectively (Fig. 1B–D). In HeLa cells expressing both *Npu*DnaE$_C$-Venus and Lyn-Ceru-*Npu*DnaE$_N$-mRFP1, the plasma membrane was cyan–yellow fluorescent, while the cytoplasm was red fluorescent because the *Npu*DnaE intein splices itself out along with mRFP1 to create a new fusion protein consisting of Cerulean and Venus (Fig. 1E–G). Similar results were obtained for COS7 and CHO cells (Supplemental Fig. 1). *Npu*DnaE intein has a remarkable structural tolerance as protein *trans*-splicing can still occur when *Npu*DnaE$_N$ is sandwiched between two relatively large, bulky fluorescent proteins (Fig. 1A). Similarly, to test the structural tolerance of the other intein half, *Npu*DnaE$_C$, the fusion proteins Lyn-Ceru-*Npu*DnaE$_N$ and mRFP1-*Npu*DnaE$_C$-Venus were constructed (Supplemental Fig. 1). In HeLa cells expressing mRFP1-*Npu*DnaE$_C$-Venus or Lyn-Ceru-*Npu*DnaE$_N$ alone, the cytoplasm was yellow–red fluorescent and the plasma membrane was cyan fluorescent, respectively (Fig. 1H–J). In HeLa cells expressing both mRFP1-*Npu*DnaE$_C$-Venus and Lyn-Ceru-*Npu*DnaE$_N$, as expected, the plasma membrane was cyan–yellow fluorescent, while the cytoplasm was red fluorescent (Fig. 1K and L). Similar imaging results were observed in COS7 and CHO cells (Supplemental Fig. 1).

2.2. NpuDnaE intein mediated protein splicing of the TN-XL Ca^{2+} indicator

In mammalian cells expressing an artificially split TN-XL biosensor fused to its respective *Npu* intein halves, there was successful protein *trans*-splicing to reassemble a functional TN-XL Ca^{2+} biosensor. TN-XL is a commonly used FRET-based Ca^{2+} biosensor composed of a chicken skeletal troponin C (TnC) sandwiched between the donor–acceptor pair, ECFP and citrine [23]. In order to minimally perturb each constituent protein, TN-XL was artificially split within the linker region separating the N-terminus ECFP and TnC-citrine. The N-terminus ECFP was then tandem fused to *Npu*DnaE$_N$ to obtain the fusion protein ECFP-*Npu*DnaE$_N$ while the TnC-citrine half was fused to *Npu*DnaE$_C$ to form the fusion protein *Npu*DnaE$_C$-TnC-citrine (Fig. 2A). The co-expression of the two split TN-XL intein constructs in mammalian cells directed protein *trans*-splicing to reconstruct the TN-XL biosensor. However, the protein *trans*-splicing process leaves behind the residual amino acids "CFNGT" with the spliced product [18,24]. As a result, the newly reassembled TN-XL biosensor is a mutant form with a longer linker region between ECFP and TnC-citrine (Fig. 2A). To assess the effectiveness of the reassembled split TN-XL biosensor, HeLa cells were either transfected with the artificially split or unaltered TN-XL biosensor (Fig. 2B, C and E, F, respectively)). Ca^{2+} transients were induced by stimulation with 50 μM UTP [25] and FRET responses from the biosensors were measured (Fig. 2D and G). Dynamic range was obtained by loading cells with ionomycin in the presence of 5 mM Ca^{2+} followed by the loading of 5 mM EDTA. The reassembled split TN-XL had a significantly reduced FRET dynamic range compared to the unaltered TN-XL biosensor (1.1 ± 0.2 and 1.7 ± 0.4, respectively with *t*-test $p < 0.001$, $n = 3$) (Fig. 2H). This reduced FRET dynamic range may be attributable to the longer linker region between ECFP and TnC-citrine at the point of protein *trans*-splicing that likely altered the orientation of the fluorophores and increased the separation distance between the fluorophores [5,26]. Similar imaging results were obtained in COS-7 and CHO cell lines (Supplemental Fig. 2).

To show the responses obtained from the reassembled split TN-XL biosensor was a result of *Npu*DnaE intein splicing activities, non-splicing construct pairs were co-expressed in mammalian cells and tested for activity. The co-expression of the fusion proteins Ceru-*Npu*DnaE$_N$ and TnC-Citrine in HeLa cells produced no measurable Ca^{2+} transients when stimulated with 50 μM UTP. Likewise, loading of ionomycin in the presence of 5 mM Ca^{2+} followed by the loading of 5 mM EDTA produced no measurable response (Supplemental Fig. 3). Correspondingly, the co-expression of ECFP and *Npu*DnaE$_C$-TnC-Citrine in HeLa cells produced no measurable Ca^{2+} response after stimulation with 50 μM UTP and loading of ionomycin in the presence of 5 mM Ca^{2+} followed by the loading of 5 mM EDTA (Supplementary Fig. 3). In theory, the split TN-XL should have the greatest dynamic range when the halves have equal stoichiometry because the amount of unpaired halves and their background fluorescence are minimized. When protein constructs were extracted from mammalian cells and separated on SDS-PAGE, it revealed the presence of unconsumed precursor proteins along with the reassembled TN-XL biosensor (Supplementary Fig. 4).

2.3. NpuDnaE intein mediated protein splicing of the GCaMP2 Ca^{2+} indicator

In mammalian cells expressing an artificially split GCaMP2 biosensor tandem fused to its respective intein halves, there was likewise successful protein *trans*-splicing to reconstruct a functional GCaMP2 biosensor. GCaMP2 is a commonly used single fluorophore intensity Ca^{2+} biosensor consisting of a tandem fusion of the calmodulin binding peptide from myosin light chain kinase, a circularly permutated EGFP (cpEGFP) and calmodulin [12,27]. Structural examination of GCaMP2 (PDB ID: 3EVR) revealed the optimal position to divide GCaMP2 with the least disturbance to its native structural arrangement was within the linker region situated between the circularly permutated EGFP (cpEGFP) [10,27]. To minimize the effects of the residual peptide sequence from protein splicing, the split GCaMP2-intein constructs were designed such that after protein splicing the residual peptide sequence, "CFNGT",

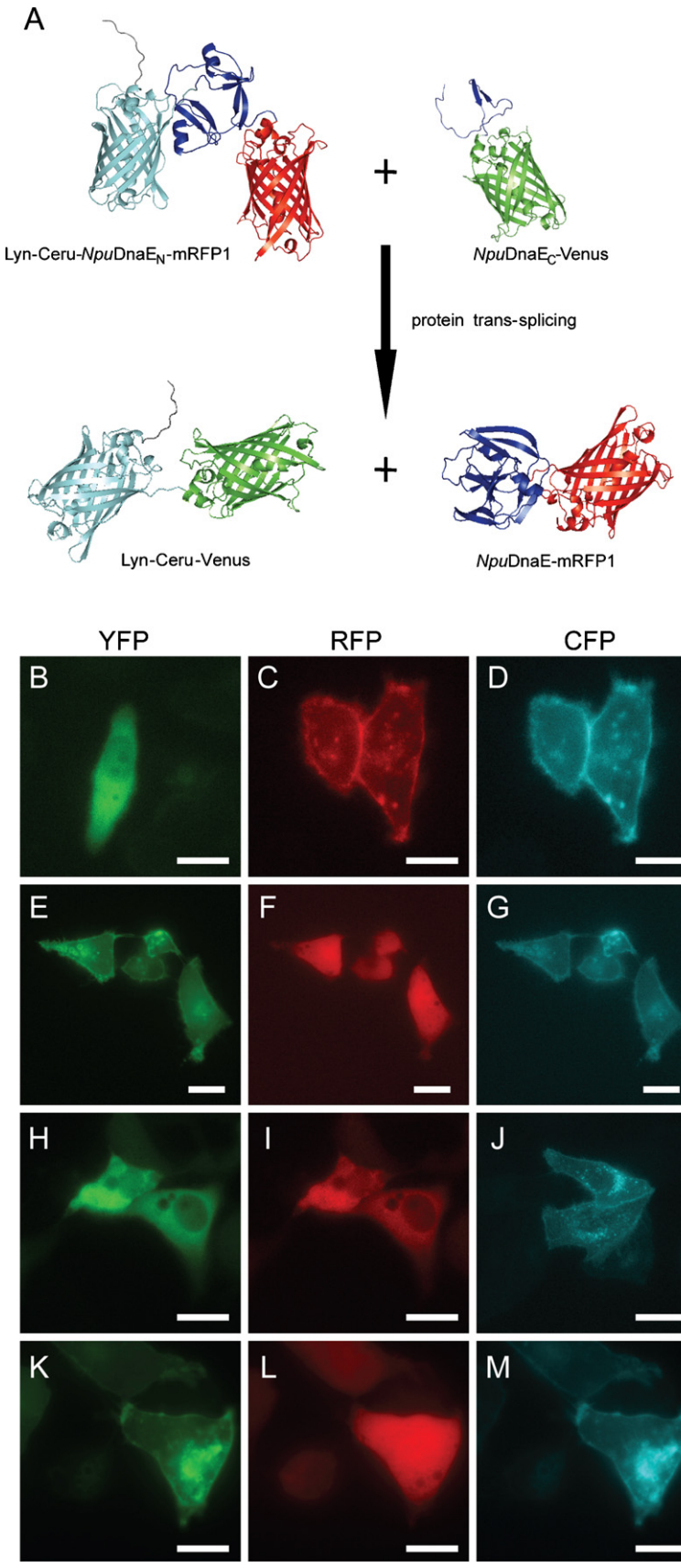

Fig. 1. *Npu*DnaE intein has splicing activity in mammalian cells. (A) Structural modeling of the protein *trans*-splicing process. The high affinity of the naturally split *Npu*DnaE intein halves (*Npu*DnaE$_N$ and *Npu*DnaE$_C$, shown in blue) for each other results in the spontaneous formation of the active intein when both halves are present. The active intein (blue) splices itself out along with mRFP1 (red) via a peptide bond linking together Cerulean (cyan) and Venus (green). The plasma membrane localizing peptide, Lyn, is shown in black. Images of HeLa cells transfected with (B) *Npu*DnaE$_C$-Venus and (C, D) Lyn-Ceru-*Npu*DnaE$_N$-mRFP1 alone, and their (E–G) co-expression. HeLa cells transfected with (H, I) mRFP1-*Npu*DnaE$_C$-Venus and (J) Lyn-Ceru-*Npu*DnaE$_N$ alone, and their (K–M) co-expression. Scale bars are 10 μm. Images are in false colour. (For interpretation of the references to colour in this figure legend, the reader is referred to the web version of the article.)

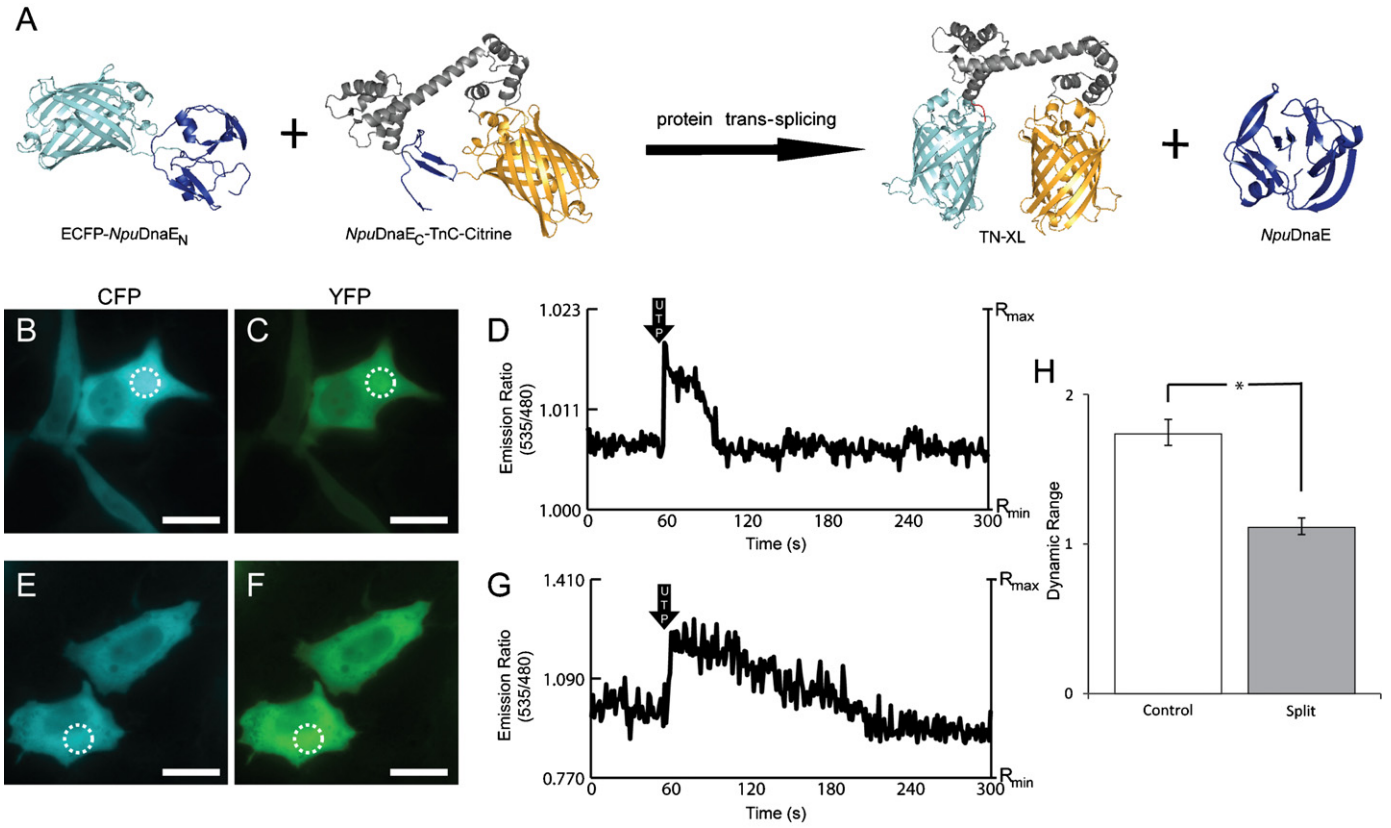

Fig. 2. Protein *trans*-splicing of split TN-XL Ca^{2+} indicator. (A) Structural modeling of protein *trans*-splicing of the split TN-XL Ca^{2+} biosensor. TN-XL was artificially split between the first fluorescent protein ECFP (cyan) and chicken skeletal troponin C (TnC, grey) and fused to its respective *Npu*DnaE intein halves (blue). The resultant product of the protein *trans*-splicing process is the reassembled TN-XL Ca^{2+} biosensor and the whole *Npu*DnaE intein (blue). Of note is the residual amino acids "CFNGT" that is incorporated into the TN-XL Ca^{2+} biosensor at the splice site (shown in red). Citrine is shown in yellow. (B) Co-expression of the two split TN-XL intein constructs in HeLa cells shown under CFP and (C) YFP fluorescence and (D) the emission ratio (535 nm/480 nm) of Ca^{2+} transients obtained from UTP stimulation. Expression of control TN-XL Ca^{2+} biosensor in HeLa cells under (E) CFP and (F) YFP fluorescence and (G) emission ratio of an UTP-induced Ca^{2+} transient. (H) Comparison of the mean dynamic range of the control and reassembled split TN-XL Ca^{2+} biosensor ($n = 3$ experiments). Scale bars are 10 μm. White dotted circle represent regions where average fluorescence intensity measurements were taken. Images are in false colour. (For interpretation of the references to colour in this figure legend, the reader is referred to the web version of the article.)

would replace the native linker sequence, "GGTGGS". This was accomplished by directly fusing RSET, a plasmid leader sequence, M13, a myosin light chain kinase fragment, and cpEGFP(149–238) to *Npu*DnaE$_N$ to form nGCaMP2-*Npu*DnaE$_N$ for the N-terminus construct while the C-terminal portion consisted of *Npu*DnaE$_C$ directly fused to cpEGFP(1–144)-CaM to form *Npu*DnaE$_C$-cGCaMP2 (Fig. 3A). To confirm that the altered GCaMP2 biosensor retained a similar activity as the unaltered GCaMP2, the altered GCaMP2 biosensor was prepared by replacing the native linker sequence with the residual peptide sequence. When expressed in mammalian cell lines, the altered GCaMP2 biosensor measured induced Ca^{2+} transients in a dynamic range that was statistically indistinguishable from the unaltered GCaMP2 biosensor (2.62 ± 0.29 and 2.75 ± 0.10, respectively with *f*-test $p = 0.02$, $n = 3$) (Supplemental Fig. 5).

HeLa cells were transfected with the artificially split or unaltered GCaMP2 biosensor and a Ca^{2+} transient was induced by UTP and measured (Fig. 3B, C and D, E). Dynamic range was again obtained by loading cells with ionomycin in the presence of 5 mM Ca^{2+} followed by the loading of 5 mM EDTA. The reassembled split GCaMP2 had a statistically indistinguishable dynamic range compared to the unaltered GCaMP2 biosensor (2.75 ± 0.41 and 2.79 ± 0.10, respectively with *f*-test $p = 0.004$, $n = 3$) (Fig. 3). Similar imaging results were also obtained in COS-7 and CHO cell lines (Supplemental Fig. 6). Notably, cells individually transfected with only nGCaMP2-*Npu*DnaE$_N$ or *Npu*DnaE$_C$-cGCaMP2 did not display any fluorescence. Thus, unpaired GCaMP2 halves do not contribute to the background fluorescence and equal stoichiometry is unnecessary. Furthermore, co-expression of non-splicing construct pairs (nGCaMP2-*Npu*DnaE$_N$ with cGCaMP2; nGCaMP2 with *Npu*DnaE$_C$-cGCaMP2) had no fluorescently labelled cells needed to perform a Ca^{2+} imaging experiment, suggesting that the reassembled split GCaMP2 activity requires intein protein-splicing. A SDS-PAGE analysis revealed the formation of the spliced products from its precursors (Supplemental Fig. 7).

2.4. Expression in pharyngeal muscle cells of C. elegans

Next, we created transgenic *C. elegans* co-expressing nGCaMP2-*Npu*DnaE$_N$ and *Npu*DnaE$_C$-cGCaMP2 (the split GCaMP2-intein constructs) under the myo-2 promoter for pharyngeal muscle cells expression (Fig. 4). The split GCaMP2 was chosen over TN-XL for two reasons: first, the dynamic range was as good as the unaltered GCaMP2; second, any unpaired partners do not contribute to background fluorescence. The pharyngeal muscles are composed of three components: the corpus, isthmus and terminal bulb [28–30]. These three components make up a relatively large (the terminal bulb alone has a diameter of around 20 μm) muscular organ involved in grinding and directing food into the worm's intestines. Because these muscle cells are electrically coupled by gap junctions, the organ gives large synchronized Ca^{2+} transients, thus easing tracking and Ca^{2+} dynamic measurements [29,30]. An automatic

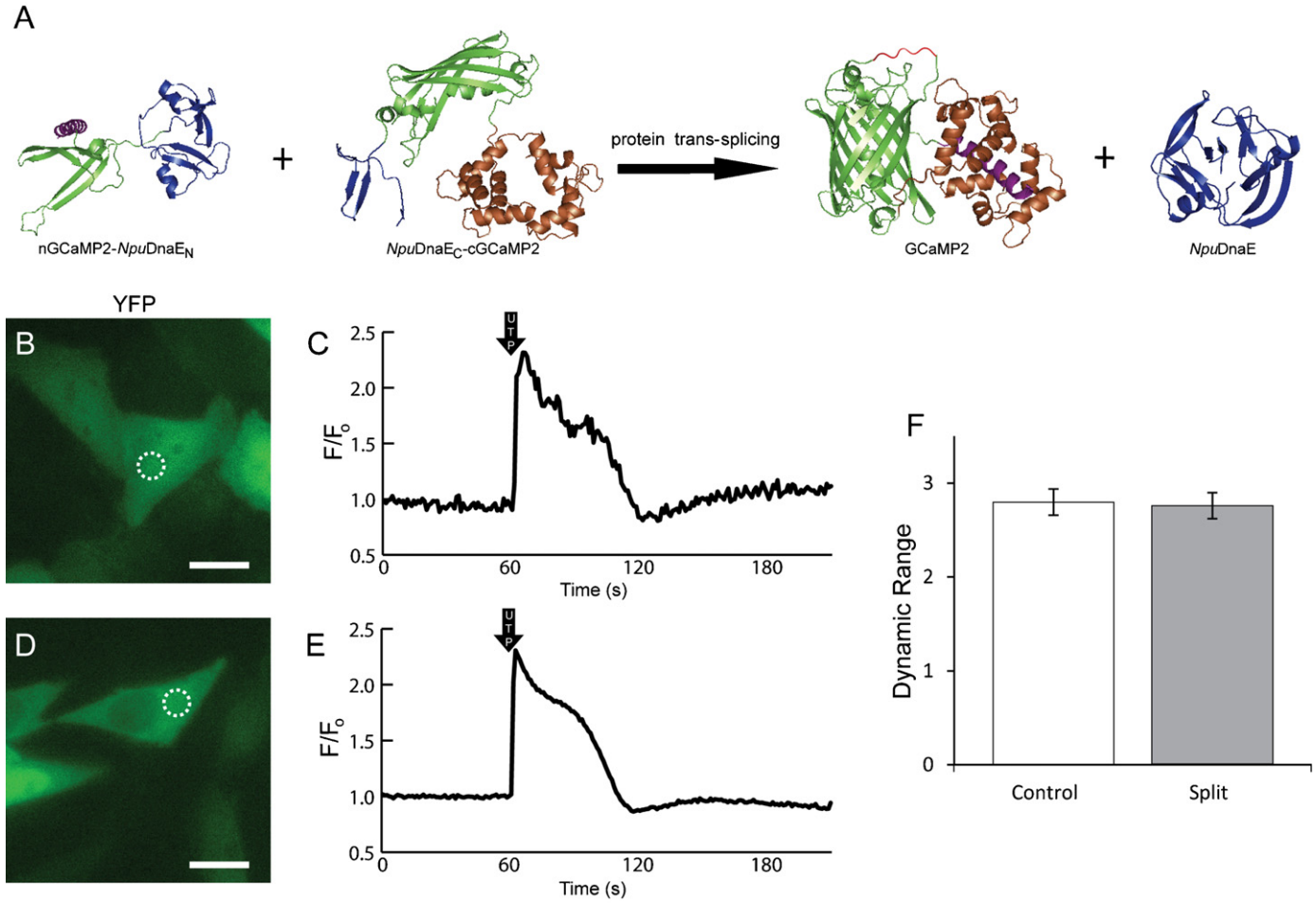

Fig. 3. Protein *trans*-splicing of split GCaMP2. (A) Structural modeling of the protein *trans*-splicing process. To split GCaMP2, the native linker region "GGTGGS" was removed and the resultant halves (EGFP in green; M13 in purple; calmodulin in brown) were fused to its respective intein halves (blue). Protein *trans*-splicing reassembled GCaMP2 and the whole *Npu*DnaE intein. However, the reassembled GCaMP2, now a mutant, has the residual peptide sequence "CFNGT" replacing the native linker (shown in red). (B) Fluorescence image of HeLa cells co-expressing the two split GCaMP2 intein constructs and (C) its UTP-induced Ca^{2+} transients as measured by the reassembled split GCaMP2. (D) Fluorescence image of HeLa cells expressing the control GCaMP2 and (E) its UTP-induced Ca^{2+} transients. (H) Comparison of mean dynamic range of control and reassembled split GCaMP2 ($n = 3$ experiments). Scale bars are 10 μm. White dotted circle represent regions where average fluorescence intensity measurements were taken. Images are in false colour. (For interpretation of the references to colour in this figure legend, the reader is referred to the web version of the article.)

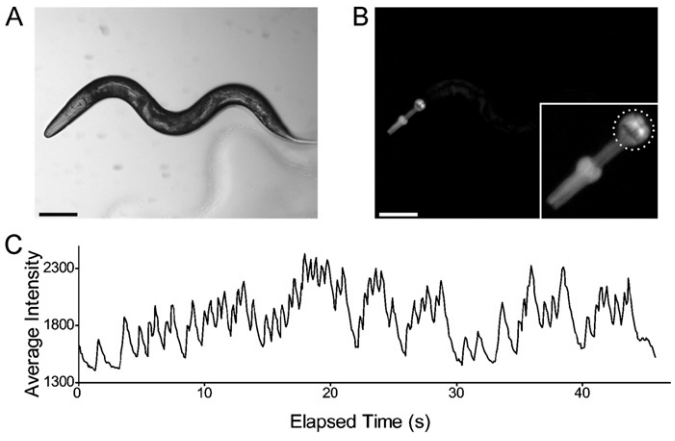

Fig. 4. Detection of Ca^{2+} transients in the pharynx of freely moving *C. elegans* using split GCaMP2. (A) The transgenic *C. elegans* co-expressing myo-2p::nGCaMP2-*Npu*DnaE$_N$ and myo-2p::*Npu*DnaE$_C$-cGCaMP2 were imaged in bright field and (B) fluorescence. The dotted circle (B, inlet) indicates the terminal bulb region of the pharynx in which the fluorescence intensity was measured for time series. (C) Normalized intensity of the terminal bulb was plotted as a function of time. The animal was stimulated with 1 mg/ml of serotonin for 10 min, and then placed on an imaging substrate for fully locomotive imaging. Scale bars represent 100 μm.

tracking system was developed to continuously track and measure the Ca^{2+} transients on freely moving worms. The transgenic worms were stimulated with serotonin to induced rapid feeding behaviour. Average fluorescence intensity of the terminal bulb was obtained by automated pattern-matching algorithm, and had similar profiles as the response from the native GCaMP2 biosensor (Supplemental Fig. 8). Transgenic *C. elegans* expressing either nGCaMP2-*Npu*DnaE$_N$ or *Npu*DnaE$_C$-cGCaMP2, but not both, did not exhibit any fluorescence when stimulated, as expected (Supplemental Fig. 9). Notably, the split GCaMP2-intein constructs were expressed in all three pharyngeal muscle regions (the corpus, isthmus, and terminal bulb). This is different from initial Ca^{2+} dynamic studies where a variant of the Ca^{2+} indicator, cameleon, was precluded from the isthmus [29], but is similar to studies using a variant of pericam [30,31].

3. Discussion

To ultimately enable cell-type specific targeting of GECIs using two promoters, we report here the artificial splitting and post-translational reassembly of two representative GECIs, TN-XL and GCaMP2, by exploiting the phenomenon of protein splicing. The naturally occurring split DnaE intein from *Nostoc punctiforme* allowed protein *trans*-splicing to occur in a foreign context in both mammalian cell lines and our animal model – *C. elegans*. *Npu*DnaE

intein was chosen as the ideal intein element because it exhibits a high-rate of protein *trans*-splicing reaction with respect to different extein sequences and allows protein *trans*-splicing to occur spontaneously when expressed, eliminating the need for exogenous factors [18,19]. An unexpected finding was the large structural tolerances of *Npu*DnaE intein. Since structural inspection of the NMR structure of *Npu*DnaE intein (PDB ID: 2KEQ) [32] revealed the close proximity of the splice sites, it would be expected that the fusion of a bulky protein would hinder protein *trans*-splicing [17,33,34]. However, two relatively large bulky fluorescent proteins (26.9 kDa) flanking both ends of either *Npu*DnaE$_N$ (11.9 kDa) or *Npu*DnaE$_C$ (4.1 kDa) had minimal effects on the *trans*-splicing activity of the intein. This further validates the remarkable robustness of the *Npu*DnaE intein.

While the split TN-XL biosensor would allow for ratiometric Ca^{2+} imaging, it had significantly diminished response relative to the native TN-XL biosensor. This was due to the residual peptide sequence after protein splicing and the unequal stoichiometry of the two halves. A significant limitation of the split TN-XL biosensor was that the expression of each precursor half is fluorescent. Thus, any unconsumed precursor constructs would contribute to background fluorescence and interfere with measuring the signal response. When two different promoters are used, this effect is further complicated as the constructs are expressed at different levels. The potentially significant background fluorescence makes the split TN-XL biosensor challenging to use in animal models. We expect other FRET-based biosensors to have similar limitations.

In contrast, the split GCaMP2 biosensor retained similar functionality when expressed in various mammalian cell lines and our animal model – *C. elegans*. In our cell line studies, the dynamic range of the reassembled GCaMP2 was indistinguishable to the native GCaMP2 biosensor. Fluctuating Ca^{2+} dynamics in contracting pharyngeal muscle cells of *C. elegans* exhibited similar profiles as studies with native calcium probes by other groups. Unlike the split TN-XL biosensor, the precursor halves of the split GCaMP2 biosensor were not fluorescent and fluorescence is only restored in those cases where protein splicing was complete. Thus, effectiveness of the biosensor is not dependent on stoichiometry of the halves and only the cell-types that are targeted will be fluorescent. These properties make split GCaMP2 biosensor a more desirable split GECI in cases where ratiometric Ca^{2+} imaging is not necessary.

4. Conclusion

We have demonstrated the ability of two representative GECIs (i.e. TN-XL and GCaMP2) to be artificially split and reassembled post-translationally back together using *Npu*DnaE intein. While both split GECIs could monitor intracellular Ca^{2+} signalling in mammalian cells, the split GCaMP2 biosensor was particularly suitable for imaging in animal models such as *C. elegans* because the precursor halves were not fluorescent. In this study, both precursor halves were under the control of the same promoter, but they could be easily engineered to two different promoters to yield cell-type specific targeting of GECIs. For instance, this could allow the previously untargetable interneurons to be studied to further our understanding of the complex and intricate signalling of neural networks in animal models.

5. Materials and methods

5.1. Plasmid construct and subcloning

*Npu*DnaE$_N$ and *Npu*DnaE$_C$ were cloned from Addgene (Cambridge, MA) plasmids 12,172 and 15,335, respectively [18]. For *Npu*DnaE$_C$, the first three amino acids of the native extein sequence were included. N- and C-terminal portions of split TN-XL and GCaMP2 were amplified by standard PCR with primers described below from their respective full length counterpart. The N-terminal portions of TN-XL and GCaMP2 were subsequently fused to the amino end of *Npu*DnaE$_N$. The C-terminal portions of TN-XL and GCaMP2 were fused to the carboxyl end of *Npu*DnaE$_C$. The substitution of the linker region "GGTGGS" with "CFNGT" in the altered GCaMP2 biosensor was created using self-hybridizing primers and inserted into cassette [35]. All subcloning were performed as previously described [35,36].

5.2. Cell culture and transfection

Cell lines (COS7, CHO, HeLa) were maintained in Dulbecco's Modified Eagle's Medium supplemented (DMEM) with 25 mM D-glucose, 1 mM sodium pyruvate, 4 mM L-glutamine (Invitrogen), 10% fetal bovine serum, and 10 mL/L penicillin–streptomycin solution (Sigma–Aldrich, St. Louis, MO, USA) in T5 flasks (37 °C and 5% CO_2). At 95% confluency, cells were passaged by washing with PBS (Invitrogen) and incubating with 1 mL of 0.05% trypsin–EDTA (Sigma–Aldrich) at 37 °C for 3–5 min. Cells were then seeded onto glass-bottom dishes (MatTek Corp.) at 1:10 dilution. Transfection was performed using Lipofectamine 2000 according to manufacturer's protocols (Invitrogen Life Technologies, Carlsbad, CA, USA). Co-transfections were verified by screening for two fluorescent proteins (ECFP and citrine; TN-XL) or diminished fluorescence of the fluorescent protein (EGFP; GCaMP2).

5.3. SDS-PAGE gel preparations

All protein constructs were expressed in either HeLa or COS7 cells. For the TN-XL intein constructs, proteins were extracted by sonication (Branson Sonifier 250) and separated on NuPage Novex 4–12% Bis–Tris Pre-cast gel with NuPage 1× SDS-MOPS buffer according to manufacturer's protocols (Invitrogen). The gel was then examined using 440/480 nm (excitation/emission) filters for ECFP fluorescence and 488/525 nm filters for Citrine fluorescence (Illumatool Lighting System, Light Tools Research, Encinitas, CA, USA). For the GCaMP2 intein constructs, extracted proteins were first purified using the native His-tag with His-Mag Purification Kit according to manufacturer's protocols (Novagen, Darmstadt, Germany). Beads were directly loaded and separated on SDS-PAGE gel. The gel was then stained overnight in PageBlue (Fermentas, Maryland, USA). Photographs were taken with a Canon A350 digital camera.

5.4. Reagents used and cell culture imaging and illumination

ATP and UTP were obtained from Fermentas and ionomycin and EDTA were from Sigma–Aldrich. To induce Ca^{2+} transients, COS7 and CHO cells were stimulated with 10 μM ATP, while HeLa cells were stimulated with 50 μM UTP. To obtain maximum and minimum values of Ca^{2+}, ionomycin and then 2.5 mM EDTA were used respective after Ca^{2+} transients were completed. All cell culture imaging experiments were performed in PBS supplemented with 5 mM $CaCl_2$ and 1 mM $MgCl_2$ (Invitrogen). Imaging was performed using an inverted IX81 microscope with Lambda DG4 xenon lamp source and QuantEM 512SC CCD camera with a 60× oil immersion objective (Olympus). FRET measurements were collected using a filter cube containing a CFP excitation filter (438/24 nm) with a dual-band filter (480/30 nm and 535/30 nm, 505 nm beam-splitter dichroic mirror, Photometrics DV2) to simultaneously collect CFP

and YFP emissions. EGFP intensity measurements were collected with QuantEM 512SC CCD.

5.5. Dynamic range data analysis

For FRET analysis, all emission ratios (535 nm/480 nm) were determined from raw time series measurements and then normalized against I_o, where I_o is the mean fluorescence intensity signal during the baseline period prior to the Ca^{2+} transient stimuli. FRET dynamic ranges were determined from R_{max}/R_{min} of FRET ratios (535 nm/480 nm). Single fluorescence intensity measurements were reported as F/F_o, where F is the raw fluorescence intensity time series minus background fluorescence, and F_o is the mean fluorescence signal in the baseline period prior to Ca^{2+} transient stimulations. To test for statistically significant differences between two sets of data points, unpaired (independent) Student's *t*-test with unequal variances was used. To test for two sets of data points that are not significantly different, *f*-test was used. In both cases, *p*-values of less than 0.05 are considered statistically significant. All values shown are mean ± standard deviation.

5.6. Tracking, imaging, and generation of transgenic C. elegans

A custom-made tracking system with a fluorescent microscope (MVX10, Olympus), a motorized stage (99S106, Ludl), a stage controller (MAC5000, Ludl), a CCD camera (CoolSNAP HQ2, Photometrics), a light source (exacte, X-cite), and custom-made MATLAB (v7.10, MathWorks) script was arranged for Ca^{2+} imaging of locomoting *C. elegans*. The fluorescence filter cube includes an excitation filter (470/40 nm, Chroma), a dichroic mirror (495 nm LP, Chroma), and an emission filter (525/50 nm, Chroma). An objective lens (MVPLAPO 2XC NA = 0.5, Olympus) and a zoom lens were combined to give 12.5× magnification power. Exposure time was 10 ms for Ca^{2+} imaging and 200 ms for still images (MetaMorph v7.14, Molecular Devices). The N-GCaMP2-*Npu*$DnaE_N$ and *Npu*$DnaE_C$-C-GCaMP2 (20 ng/μl each) plasmids were co-injected to the distal gonads of N_2 worms to induce extra chromosomal expression of the split GCaMP2 genes. All genes were under the control of the myo-2 promoter for expression in pharyngeal muscle cells. Fluorescent animals with uniform expression pattern among the pharyngeal muscles were selected for imaging. The transgenic animals were submerged in 1 mg/ml serotonin solution (H7752, Sigma) for 10 minutes, and then transferred to a 2% agarose (15517-022, Invitrogen) pad with buffer (50 mM NaCl, 10 mM HEPES–NaOH pH 7.1, 1 mM $CaCl_2$ and 1 mM $MgSO_4$) for imaging.

Conflict of interest

There are no conflict of interests.

Acknowledgments

This work was supported by a grant to KT and HS from the Canadian Institutes of Health Research (#81262 and #97902, respectively). SW designed and carried out the experiments, created plasmids used, analyzed the data and wrote the manuscript. IK and HS created the transgenic worms, performed Ca^{2+} imaging and analyzed the data. EM produced plasmids used in the work. KT conceived the initial idea, analyzed the data and helped write the manuscript.

Appendix A. Supplementary data

Supplementary data associated with this article can be found, in the online version, at doi:10.1016/j.ceca.2011.10.006.

References

[1] R.W. Tsien, Calcium channels, stores, and oscillations, Annual Review of Cell Biology 6 (1990) 715–760.
[2] D.E. Clapham, Calcium signaling, Cell 80 (1995) 259–268.
[3] M.J. Berridge, M.D. Bootman, P. Lipp, Calcium – a life and death signal, Nature 395 (1998) 645–648.
[4] M.J. Berridge, M.D. Bootman, H.L. Roderick, Calcium signalling: dynamics, homeostasis and remodelling, Nature Reviews Molecular Cell Biology 4 (2003) 517–529.
[5] M. Mank, O. Griesbeck, Genetically encoded calcium indicators, Chemical Reviews 108 (5) (2008) 1550–1564.
[6] R. Rudolf, et al., Looking forward to seeing calcium, Nature Reviews Molecular Cell Biology 4 (2003) 579–586.
[7] R.Y. Tsien, Imagining imaging's future, Nature Reviews Molecular Cell Biology 4 (2003) SS16–SS21.
[8] M.I. Kotlikoff, Genetically encoded Ca^{2+} indicators: using genetics and molecular design to understand complex physiology, Journal of Physiology 578 (1) (2007) 55–67.
[9] L. Tian, et al., Imaging neural activity in worms: flies and mice with improved GCaMP calcium indicators, Nature Methods 6 (12) (2009) 875–881.
[10] G.S. Baird, D.A. Zacharias, R.Y. Tsien, Circular permutation and receptor insertion within green fluorescent proteins, Proceedings of the National Academy of Sciences of the United States of America 96 (1999) 11241–11246.
[11] A. Miyawaki, et al., Fluorescent indicators for Ca^{2+} based on green fluorescent proteins and calmodulin, Nature 388 (1997) 882–887.
[12] Y.N. Tallini, et al., Imaging cellular signals in the heart in vivo: Cardiac expression of the high-signal Ca^{2+} indicator GCaMP2, Proceedings of the National Academy of Sciences of the United States of America 103 (12) (2006) 4753–4758.
[13] C. Zheng, B.J. Baum, Evaluation of promoters for use in tissue-specific gene delivery, Methods in Molecular Biology 434 (2008) 205–219.
[14] I. Ghosh, A.D. Hamilton, L. Regan, Antiparallel leucine zipper-directed protein reassembly: application to the green fluorescent protein, Journal of American Chemical Society 122 (2000) 5658–5659.
[15] R.Y. Tsien, The green fluorescent protein, Annual Review of Biochemistry 67 (1998) 509–544.
[16] S. Zhang, C. Ma, M. Chalfie, Combinatorial marking of cells and organelles with reconstituted fluorescent proteins, Cell 119 (1) (2004) 137–144.
[17] L. Saleh, F.B. Perler, Protein splicing in cis and in trans, The Chemical Record 6 (2006) 183–193.
[18] H. Iwai, et al., Highly efficient protein trans-splicing by a naturally split DnaE intein from Nostoc punctiform, FEBS Letters 580 (7) (2006) 1853–1858.
[19] J. Zettler, V. Schutz, H.D. Mootz, The naturally split Npu DnaE intein exhibits an extraordinary high rate in the protein trans-splicing reaction, FEBS Letters 583 (5) (2009) 909–914.
[20] T. Nagai, et al., A variant of yellow fluorescent protein with fast and efficient maturation for cell-biological applications, Nature Biotechnology 20 (2002) 87–90.
[21] M.A. Rizzo, et al., An improved cyan fluorescent protein variant useful for FRET, Nature Biotechnology 22 (4) (2004) 445–449.
[22] R.E. Campbell, et al., A monomeric red fluorescent protein, Proceedings of the National Academy of Sciences of the United States of America 99 (12) (2002) 7877–7882.
[23] M. Mank, et al., A FRET-based calcium biosensor with fast signal kinetics and high fluorescence change, Biophysical Journal 90 (2006) 1790–1796.
[24] S.W. Lockless, T.W. Muir, Traceless protein splicing utilizing evolved split inteins, Proceedings of the National Academy of Sciences of the United States of America 106 (27) (2009) 10999–11004.
[25] L. Welter-Stahl, et al., Expression of purinergic receptors and modulation of $P2X_7$ function by the inflammatory cytokine IFN_γ in human epithelial cells, Biochimica et Biophysica Acta: Biomembranes 1788 (5) (2009) 1176–1187.
[26] E.A. Jares-Erijman, T.M. Jovin, FRET imaging, Nature Biotechnology 21 (2003) 1387–1395.
[27] Q. Wang, et al., Structural basis for calcium sensing by GCaMP2, Structure 16 (2008) 1817–1827.
[28] D.G. Albertson, J.N. Thomson, The pharynx of *Caenorhabditis elegans*, Philosophical Transaction of the Royal Society of London 275 (1975) 299–325.
[29] R. Kerr, et al., Optical imaging of calcium transients in neurons and pharyngeal muscle of *C. elegans*, Neuron 26 (2000) 583–894.
[30] S. Shimozono, et al., Slow Ca^{2+} dynamics in pharyngeal muscles in *Caenorhabditis elegans* during fast pumping, European Molecular Biology Organization 5 (5) (2004) 521–526.
[31] T. Nagai, et al., Circularly permutated green fluorescent proteins engineered to sense Ca^{2+}, Proceedings of the National Academy of Sciences of the United States of America 98 (6) (2001) 3197–3202.
[32] J.S. Oeemig, et al., Solution structure of DnaE intein from Nostoc punctiforme: structural basis for the design of a new split intein suitable for site-specific chemical modification, FEBS Letters 538 (9) (2009) 1451–1456.

[33] H. Paulus, Protein splicing and related forms of protein autoprocessing, Annual Review of Biochemistry 69 (2000) 447–496.
[34] Y. Anraku, R. Mizutani, Y. Satow, Protein splicing: Its discovery and structural insight into novel chemical mechanisms, IUBMB Life 57 (8) (2005) 563–574.
[35] K. Truong, A. Khorchid, M. Ikura, A Fluorescent cassette-based strategy for engineering multiple domain fusion proteins, BME Biotechnology 3 (1) (2003) 1–8.
[36] S.S.C. Wong, K. Truong, Fluorescent protein-based methods for on-plate screening of gene insertion, PLoS One 5 (12) (2010) 1–5.